

- Sandalls, *ibid.*, p. 65; O. Karlberg, *ibid.*, p. 75.
18. F. W. Whicker and T. B. Kirchner, *Health Phys.* **52**, 717 (1987).
 19. Y. C. Ng, personal communication.
 20. International Commission on Radiological Protection (ICRP), *ICRP Publication* 30, Part 1 (1979), Part 2 (1980), Part 3 (1981) (Pergamon, New York).
 21. M. D. Otis, thesis, Colorado State University, Fort Collins (1983).
 22. A. C. Chamberlain, *Atmos. Environ.* **4**, 57 (1970).
 23. If $\mu w \ll 1$, the equation reduces to $1 - p = 1 - \mu w$, or $\mu = p/w$.
 24. "Report on the National Institutes of Health Ad Hoc Working Group to develop radioepidemiological tables" (NIH Publ. 85-2748, National Institutes of Health, Washington, DC, 1985).
 25. "Health effects model for nuclear power plant accident consequence analysis" [NUREG/CR-4214 (SAND85-7185), Contractor Report, Nuclear Regulatory Commission, Washington, DC, 1985].
 26. *Genetic and Somatic Effects of Ionizing Radiation* (United Nations Scientific Committee on the Effects of Atomic Radiation, New York, 1986).
 27. *New International Atlas* (Rand McNally, New York, 1983).
 28. Some difference is expected among the countries as the time of arrival of the plume will affect the relative radionuclide mixture and the relative importance of different pathways.
 29. M. Goldman, *Science* **238**, 622 (1987).
 30. M. Otake and W. J. Schull, *Br. J. Radiol.* **57**, 409 (1984).
 31. M. Otake, H. Yoshimaru, W. J. Schull, "Severe mental retardation among the prenatally exposed survivors of the atomic bombing of Hiroshima and Nagasaki: A comparison of the T65DR and DS86 dosimetry systems" (Tech. Rep. RERF TR 16-87, Radiation Effects Research Foundation, Japan, 1987).
 32. Discussion in Proceedings of the Scientific Conference on the Medical Aspects of the Chernobyl Accident, Kiev, 11 to 13 May 1988 (Ministry of Public Health, Moscow, in press).
 33. A. I. Kondrusev, "Sanitary and hygienic measures aimed at liquidation of the Chernobyl accident consequences," in Proceedings of the Scientific Conference on the Medical Aspects of the Chernobyl Accident, Kiev, 11 to 13 May 1988 (Ministry of Public Health, Moscow, in press).
 34. A. E. Romanenko, "Public health service under conditions of a severe nuclear accident," in Proceedings of the Scientific Conference on the Medical Aspects of the Chernobyl Accident, Kiev, 11 to 13 May 1988 (Ministry of Public Health, Moscow, in press).
 35. In terms of collective dose commitment and population size, the Soviet populations within the 30-km area around the plant are not markedly different from those under study at Hiroshima and Nagasaki. The former constitute a unique research resource regarding possible lower dose-risk responses from protracted doses different from the Japanese experience. Possibly related to the dose protraction is an apparent increase in the estimated median lethal dose for the Chernobyl population (3) as compared to that for the Japanese.
 36. R. S. Cambray *et al.*, *Nucl. Energy* **26** (2), 77 (1987).
 37. B. Sorensen, *Nucl. Saf.* **28**, 443 (1987).
 38. A. Aarkrog, *J. Environ. Radioact.* **6**, 151 (1988).
 39. This work was performed under the auspices of the Department of Energy by the Lawrence Livermore National Laboratory, Livermore, CA (contract no. W-7405-Eng-48) and the University of California, Davis (contract no. DE-AC-76 SF00472), and under the auspices of the Electric Power Research Institute, Palo Alto, CA.

Chemistry of High-Temperature Superconductors

A. W. SLEIGHT

Spectacular advances in superconductors have taken place in the past two years. The upper temperature for superconductivity has risen from 23 K to 122 K, and there is reason to believe that the ascent is still ongoing. The materials causing this excitement are oxides. Those oxides that superconduct at the highest temperatures contain copper-oxygen sheets; however, other elements such as bismuth and thallium play a key role in this new class of superconductors. These superconductors are attracting attention because of the possibility of a wide range of applications and because the science is fascinating. A material that passes an electrical current with virtually no loss is more remarkable when this occurs at 120 K instead of 20 K.

SUPERCONDUCTIVITY WAS FIRST DISCOVERED IN MERCURY metal in 1911. The temperature at which mercury becomes superconducting (T_c) is 4.1 K, very close to the boiling point of liquid helium. Subsequently, other materials were discovered to be superconducting, with the highest T_c 's generally in the intermetallic compounds of niobium (1). A slow but steady rise of highest T_c took place resulting in a T_c of 23 K for Nb₃Ge in 1975 (Fig. 1).

Subsequently, a period of some disenchantment set in, reinforced by theoretical predictions that T_c would never rise above 30 K.

The field of oxide superconductors starts in the early 1960s (Fig. 1 and Table 1) (2-14). Oxides are not generally viewed as having good metallic properties although some such as ReO₃ and RuO₂ are excellent metals. On the other hand, we know that superconductors when above T_c generally do not possess the properties of good metals. The first oxides found to be superconducting were NbO and TiO (2). These oxides however may be viewed merely as metals which have dissolved some oxygen. They have NaCl-related struc-

Table 1. History of oxide superconductors.

Compound	T_c	Date discovered	Reference
TiO, NbO	1 K	1964	(2)
SrTiO _{3-x}	0.7 K	1964	(3)
Bronzes			
A _x WO ₃	6 K	1965	(4)
A _x MoO ₃	4 K	1969	(5)
A _x RcO ₃	4 K	1969	(5)
Ag ₇ O ₈ X	1 K	1966	(6)
LiTi ₂ O ₄	13 K	1974	(7)
Ba(Pb,Bi)O ₃	13 K	1975	(8)
(La,Ba) ₂ CuO ₄	35 K	1986	(9)
YBa ₂ Cu ₃ O ₇	95 K	1987	(10)
Bi/Sr/Cu/O	22 K	1987	(11)
Bi/Sr/Ca/Cu/O	90 K	1987	(12)
Tl/Ba/Ca/Cu/O	122 K	1988	(13)
K/Ba/Bi/O	30	1988	(14)

The author is with the Central Research and Development Department, E. I. du Pont de Nemours & Company, Experimental Station, Wilmington, DE 19898.

tures, but the direct metal-metal interactions are sufficiently strong to produce metallic properties. For the other oxide superconductors, the direct metal-metal interaction is too weak to give metallic properties such as high conduction (15). Instead, the conduction band is based on strong covalent bonding between oxygen and a metal. Initially, all such oxide superconductors were based on transition metal cations having an average of a fraction of one d electron per cation (16). For example, $\text{Na}_{0.2}\text{WO}_3$ has 0.2 $5d$ electron that is delocalized in a conduction band made up of W $5d$ and O $2p$ states. A breakthrough occurred when superconductivity at 13 K was found in the $\text{BaPb}_{1-x}\text{Bi}_x\text{O}_3$ system (17). It was now evident that superconductivity could also occur in oxides where there were on average a fraction of one s electron per cation. For $\text{BaPb}_{0.7}\text{Bi}_{0.3}\text{O}_3$, there are 0.3 $6s$ electrons per Pb-Bi atom; alternately, the $6s$ conduction band is 30% occupied. In retrospect, we might have expected from symmetry considerations that a fraction of one electron in a d band could be equivalent to a fraction of one hole in a d band and that thus certain oxides of copper and silver might also be superconducting. In fact, we already had examples of superconductivity in the $\text{Ag}_7\text{O}_8\text{X}$ phases in 1966 (6). It has taken twenty years to extend this concept to the oxides of copper.

Oxidation States

The chemistry of oxide superconductors cannot be discussed without reference to oxidation states. The system of oxidation states forms the cornerstone of systematics for inorganic chemistry. The term oxidation state is based on the nature of bonding of oxygen in compounds. By definition, the oxidation state of oxygen in compounds is two (O^{-II}), unless oxygen forms discrete bonds to itself, for example peroxide, $\text{O}^{-I}-\text{O}^{-I}$. Oxidation states are equivalent to real charges for the case of 100% ionicity, but no real compounds

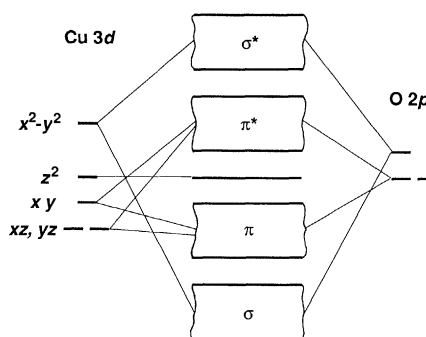


Fig. 2. Schematic energy levels for copper in square planar coordination.

are 100% ionic. In fact, even in the highly ionic oxide MgO , the real charges on Mg and O are reduced to about +1.5 and -1.5. In highly covalent oxides, the real charge on oxygen is actually less than one; nonetheless, the oxidation state remains -II by definition. Oxidation states are not real charges rounded to the nearest integer or even real charges rounded to the next highest integer. Instead, the oxidation states form a system whereby chemists predict which ratios of elements will form compounds and can also predict much about the structure and properties of such compounds. There would be no systematics for inorganic chemistry if it were not for the concept of oxidation states, equivalent to valence states. Real charges on cations and anions have no such value, but they can be calculated through the system of electronegativity. Real charges are represented here as arabic superscripts, for example, $\text{O}^{-1.1}$. Oxidation states are represented as Roman numerals, for example Cu^{III} ; they may not take on fractional values, but mixed valency (for example $\text{Cu}^{II,III}$) is possible.

There is no inconsistency in describing the oxidized copper oxides both as $\text{Cu}^{III}-\text{O}^{-II}$ and as $\text{Cu}^{+2}-\text{O}^{-1}$. The former is the correct oxidation state representation; the latter is the real charge representation where the superscripts have been rounded off partly because they are never accurately known. Both of these representations have their place. The oxidation state representation is used in this article because the definition is clearer. Nonetheless, it needs to be recognized that the real charges on both Cu^{III} and O^{-II} are in fact some noninteger values less than two.

Chemistry of Copper, Silver, and Gold

Copper, silver, and gold are in the same column of the periodic table and thus have similarities in their chemistries. They all possess both the univalent and trivalent oxidation states, for example, Cu^I , Au^{III} . The environment in the trivalent state is normally square planar for very well understood reasons (17). The common coordination of the univalent state in oxides is two-fold linear, again for well understood reasons (17). Note, however, that four-fold coordination of Cu^I and Ag^I is also well known (18). The divalent state, for example, Ag^{II} , is yet another oxidation state that can exist for this series of coinage metals, but the stability of the divalent state decreases on going down the column Cu, Ag, Au. In fact, AgO must be represented as $\text{Ag}^I\text{Ag}^{III}\text{O}_2$, and Au^{II} rarely exists except where it forms a bond to itself. On the other hand, Cu^{II} is so stable relative to disproportionation that compounds containing mixtures of Cu^I and Cu^{III} have not been well established. Nonetheless, we should expect that the tendency for Cu^{II} to disproportionate will be enhanced by high covalency of Cu-O bonds which in turn is enhanced by the presence of highly electropositive cations such as Ba^{II} (19). There is in fact evidence that $\text{YBa}_2\text{Cu}_3\text{O}_{6.5}$ contains both Cu^I and Cu^{III} as well as Cu^{II} (20).

Divalent copper usually forms four short bonds to O^{-II} which are

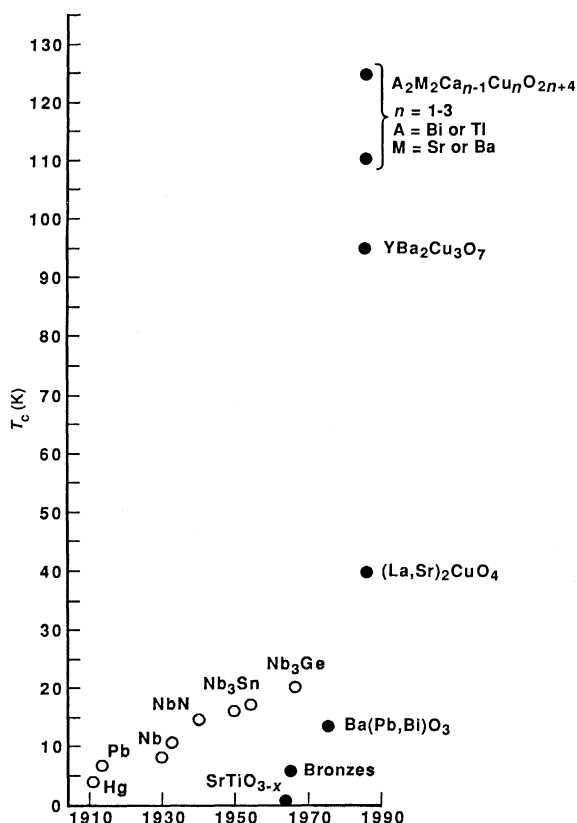


Fig. 1. Highest T_c versus date.

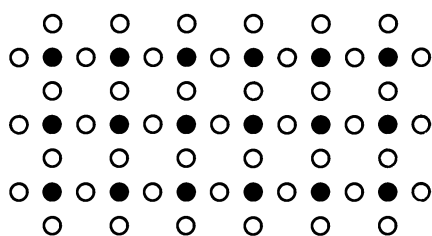


Fig. 3. The Cu-O sheet common to all copper-oxide superconductors. Open circles are oxygen, filled circles are copper.

nearly coplanar with Cu^{II} . However, it is also common to have a fifth oxygen ligand to Cu^{II} forming a square pyramidal coordination or a fifth and sixth oxygen forming a distorted octahedron. The fifth and sixth oxygens are normally at longer distances.

A schematic energy level diagram for a square planar $\text{Cu}^{\text{II}}\text{O}_4$ unit is given in Fig. 2. This is simply the molecular orbital diagram chemists would anticipate, but with the energy levels broadened into bands because of the "infinite" nature of a solid. Although there have been some suggestions (21) that the π^* level can be higher than the σ^* level, most calculations have confirmed the general features indicated in Fig. 2. I will refer to this band simply as the conduction band, not as a Cu 3d band or as an O 2p band. In fact, it is essential to emphasize that this band only exists as a result of a strong admixture of the Cu 3d and O 2p wave functions. Strictly speaking, there are no Cu 3d bands or O 2p bands in the copper oxide-based phases.

Because the conduction band shown in Fig. 2 is half filled, we might have expected metallic properties as predicted by band structure calculations. However, at present only insulating or semiconducting properties are observed at this half-filled condition. This localized behavior is now presumed to be related to high interatomic electron correlations that also result in antiferromagnetism.

As one removes electrons from the conduction band, metallic properties frequently, but not always, develop. If the metallic properties develop, superconductivity also usually occurs. If the conduction band was a broad band which supported metallic conductivity at the half-filled level, we would not be much concerned about whether the states depopulated were Cu 3d or O 2p on removal of electrons from this band. In fact, the holes are delocalized and must spend time on both Cu and O. Whether the holes spend more time on Cu or O can depend on structural details such as the Cu-O distance. I shall return to this question later in the discussion of mechanisms for superconductivity.

The basic building blocks for oxides of Cu^{II} and Cu^{III} are thus CuO_4 units that may be isolated as in Bi_2CuO_4 , or these CuO_4 units may share corners or edges to form infinite structures. The resulting structures tend to be sheets or chains (or both) of linked CuO_4 units. Three-dimensional structures of corner shared CuO_4 units are not possible with a Cu-O-Cu angle close to 180° . However, a three-dimensional structure of corner linked AgO_4 units is known in $\text{Ag}_7\text{O}_8\text{X}$ phases (6), but the Ag-O-Ag angle is now about 120° . The $\text{Ag}_7\text{O}_8\text{X}$ phases are superconducting but with T_c 's of only 1 to 2 K; thus, there is reason to suspect that a M-O-M angle close to 180° is favorable for high T_c superconductivity.

One of the simplest methods of connecting CuO_4 units together forms the infinite sheets shown in Fig. 3. This sheet is present in all the Cu-O based superconductors. As shown (Fig. 3), this sheet is a perfectly flat, square network. In fact, the sheet is normally distorted from this ideal structure in the high T_c superconductors. The square network then reduces to a rectangular network, and the oxygen is slightly out of the copper plane. The oxygen atoms may be all to one side of the Cu plane as they are in $\text{YBa}_2\text{Cu}_3\text{O}_7$, $\text{Tl}_2\text{Ba}_2\text{CaCu}_2\text{O}_8$, and $\text{Bi}_2\text{Sr}_2\text{CaCu}_2\text{O}_8$, or the oxygen may be alternately above and below the copper plane as in La_2CuO_4 and $\text{Bi}_2\text{Sr}_2\text{CuO}_6$. The Cu-O sheets

are perfectly flat and square in the case of R_2CuO_4 phases where $\text{R} = \text{Pr}, \text{Nd}, \text{Sm}, \text{and Gd}$. However, these phases are not metallic or superconducting even when doped. (22).

The bending of Cu-O-Cu bonds and resulting buckling of the Cu-O sheets may well be of importance to superconducting properties. In the ionic limit, the Cu-O sheets composed of ions would be expected to be flat and square. However, the $\text{Cu}^{\text{II}}\text{O}^{\text{II}}$ bond is highly covalent and the strongly antibonding nature of the π bond cannot be ignored. This antibonding interaction is strongest for 180° Cu-O-Cu angle and is relaxed as the bond angle bends away from 180° . The principle is the same as for an ether, where the π^* interaction between the p orbitals on carbon and oxygen force a bent C-O-C bond angle. For the Cu-O-Cu bond, it is a π^* interaction between oxygen p orbitals and Cu filled 3d orbitals. When the Cu-O-Cu bond is close to 180° , it is unstable and exhibits soft-mode behavior (23). There are various reasons to believe soft-mode behavior of the Cu-O-Cu bond could be related to superconductivity. The orthorhombic-to-tetragonal transition of La_2CuO_4 is driven by the bending of Cu-O-Cu bonds. Substitutions of the type $\text{La}_{2-x}\text{A}_x\text{CuO}_4$, where A is Ba, Sr, Ca, or Na (24), produce metallic properties and superconductivity but they also lower the orthorhombic-to-tetragonal transition temperature. As this transition temperature decreases, T_c increases. However, when the tetragonal phase becomes stable at all temperatures, superconductivity disappears. It is thus tempting to believe that the mechanism for superconductivity involves coupling to the soft mode of the Cu-O-Cu bond bending. However, this conclusion is complicated by the fact that the Cu^{III} concentration also increases with increasing x.

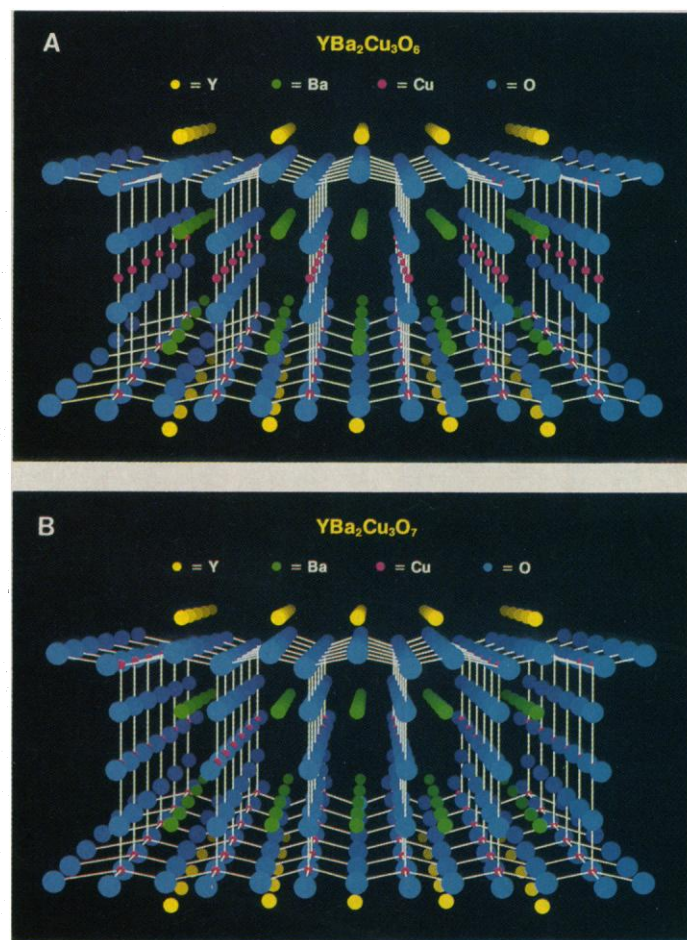


Fig. 4. The structures of (A) $\text{YBa}_2\text{Cu}_3\text{O}_6$ and (B) $\text{YBa}_2\text{Cu}_3\text{O}_7$.

With very high covalency of Cu–O bonds, the Cu–O–Cu bond bends further from 180° to produce completely different structures (25). This gives us the hope for three-dimensional structures such as found in $\text{Ag}_7\text{O}_8\text{X}$ phases where the Ag–O bonds are more covalent than Cu–O bonds. Although strong three-dimensional bonding gives rise to some very desirable properties, present evidence suggests that the bent bonds required result in lower T_c .

$\text{RBa}_2\text{Cu}_3\text{O}_{6+x}$ Phases

The structural chemistry of $\text{YBa}_2\text{Cu}_3\text{O}_{6+x}$ phases is best understood by first examining $\text{YBa}_2\text{Cu}_3\text{O}_6$. This compound is an antiferromagnetic insulator, and we may indicate the oxidation states as $\text{Y}^{\text{III}}\text{Ba}_2^{\text{II}}\text{Cu}_2^{\text{II}}\text{Cu}^{\text{I}}\text{O}_6$. The structure (Fig. 4) may be viewed as the infinite $\text{Cu}^{\text{II}}\text{O}$ sheets of Fig. 3 propped apart by $\text{O}-\text{Cu}^{\text{I}}-\text{O}$ sticks with Cu^{I} in its favored two-fold linear coordination. The oxygen from these sticks brings the Cu^{II} coordination in the sheets up to five, but this fifth Cu–O distance is considerably longer than the four forming the square around copper.

Thermodynamic stability is greatest for $\text{YBa}_2\text{Cu}_3\text{O}_{6+x}$ phases where x is close to zero; however, under most synthesis conditions x is already about 0.3. When $\text{YBa}_2\text{Cu}_3\text{O}_6$ is annealed in an oxygen-containing atmosphere at about 400°C, it acquires oxygen to form $\text{YBa}_2\text{Cu}_3\text{O}_7$ which is metallic and superconducting with a T_c of about 95 K. Compounds prepared by such intercalation reactions are generally not thermodynamically stable phases, and there is compelling evidence that $\text{YBa}_2\text{Cu}_3\text{O}_7$ is not thermodynamically stable at any condition of pressure and temperature (26). Thus the

synthesis of $\text{YBa}_2\text{Cu}_3\text{O}_7$ requires two steps: first, $\text{YBa}_2\text{Cu}_3\text{O}_{6+x}$ (small x) is formed; and second, oxidation to $\text{YBa}_2\text{Cu}_3\text{O}_7$ is carried out at a lower temperature. Although synthesis of $\text{YBa}_2\text{Cu}_3\text{O}_{6+x}$ is normally carried out at about 900°C, this temperature may be decreased to about 650°C if the oxygen partial pressure is lowered to prevent x from becoming too large (27). There have been reports of low-temperature one-step synthesis of thin films. However, the effective surface temperature of a growing film is generally much higher than the substrate temperature. Thus, the two synthesis steps may take place in one continuous process. Still one cannot rule out the possibility of directly synthesizing a metastable film as is currently being accomplished with diamond. In such cases, the results are dependent on the nature of the substrate.

When oxygen diffuses into $\text{YBa}_2\text{Cu}_3\text{O}_6$ to form $\text{YBa}_2\text{Cu}_3\text{O}_7$, the $\text{O}-\text{Cu}-\text{O}$ sticks are converted to square planar CuO_4 units that share corners to form chains (Fig. 4). It was thought that these chains somehow caused the unusually high T_c in these materials. However, we now have materials with higher T_c 's and without Cu–O chains. The oxidation states of $\text{YBa}_2\text{Cu}_3\text{O}_7$ may be written as $\text{YBa}_2\text{Cu}_2^{\text{II}}\text{Cu}^{\text{III}}\text{O}_7$. To a crude approximation, we could say that Cu in the sheets has remained divalent and that the Cu in the chains is Cu^{III} . However, both the sheets and the chains now have delocalized electron behavior and both should be represented as having the Cu^{II} , Cu^{III} mixed states.

The tetragonal symmetry of $\text{YBa}_2\text{Cu}_3\text{O}_6$ is destroyed by the chain formation along either the a or b axis. Since the a and b cell dimensions are no longer equal to each other, a crystallite undergoing this oxidation and symmetry reduction would have to change shape if it were to remain a single crystal. This is energetically

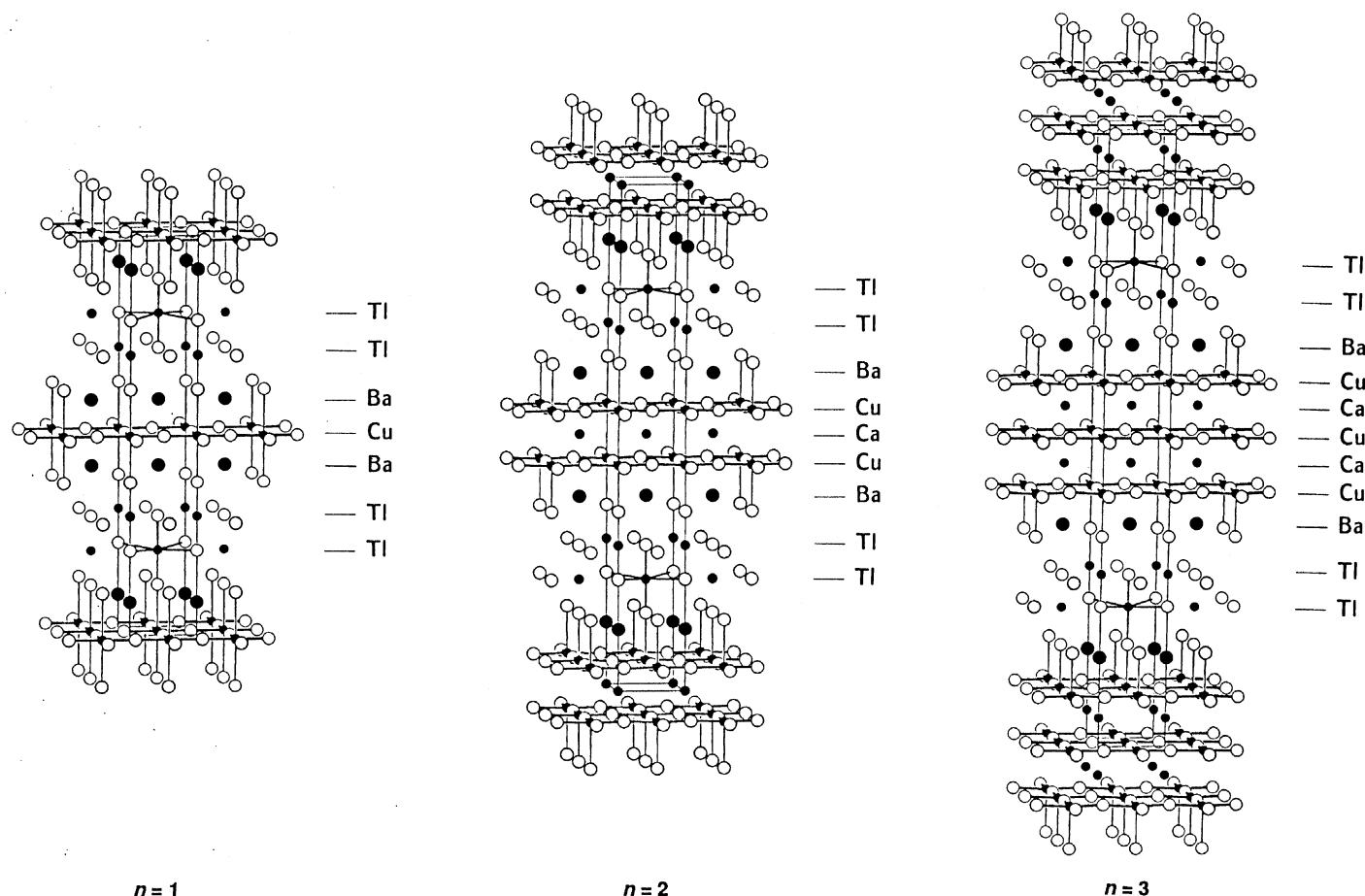


Fig. 5. The structures of $(\text{TlO})_2\text{Ba}_2\text{Ca}_{n-1}\text{Cu}_n\text{O}_{2n+2}$ for $n = 1, 2$, and 3.

unfavorable relative to formation of twins whereby the Cu–O chains run alternately along the *a* and *b* axes of the original tetragonal cell. The chains then intersect at 110 planes, and the twinning reduces the strain that would otherwise result during a crystallite shape change.

The $\text{YBa}_2\text{Cu}_3\text{O}_{6+x}$ system has been extensively studied for values of *x* from 0.0 to 1.0. The T_c decreases as *x* decreases from 1.0, but the details depend very much on synthesis conditions (28). The position of the interstitial oxygen, as well as its concentration, affect T_c . Electron diffraction studies show various superstructures that are presumably related to ordering of the oxygen interstitials (29). Indeed, a series of discrete phases has been proposed between the limiting compositions $\text{YBa}_2\text{Cu}_3\text{O}_7$ and $\text{YBa}_2\text{Cu}_3\text{O}_6$ (28, 30). The details of these structures have not been elucidated primarily because the structures are well ordered only in the two dimensions perpendicular to the *c* axis. Nonetheless, structures can be proposed based on the guiding principle that Cu atoms coordinated to only three oxygens must be kept to a minimum. Thus, there is always a tendency to form chains even for low values of *x*. A finite *x* value will then destroy the tetragonal symmetry of $\text{YBa}_2\text{Cu}_3\text{O}_6$ on a local basis (31). Presumably, fragments of chains start forming at low values of *x* and grow as oxygen content increases. The local symmetry is no longer tetragonal, but the average symmetry of many unit cells as measured by diffraction experiments remains tetragonal until the chains become sufficiently organized to all align in the same direction. In some systems, $\text{La}_{1+y}\text{Ba}_{2-y}\text{Cu}_3\text{O}_{6+x}$, for example, essentially complete formation of chains apparently occurs within a given sheet, but the chains run randomly in different directions in the different sheets (32). Therefore, there is an average tetragonal symmetry with well developed Cu–O chains.

Although $\text{YBa}_2\text{Cu}_3\text{O}_{6+x}$ phases can exist over the entire region from *x* = 0.0 to 1.0, there is no convincing evidence that such phases can exist for lower or higher oxygen contents, such as $\text{YBa}_2\text{Cu}_3\text{O}_8$. All attempts to oxidize $\text{YBa}_2\text{Cu}_3\text{O}_{6+x}$ phases beyond *x* = 1.0 have led to the destruction of this structure. There is no difficulty oxidizing more copper to the trivalent state. Indeed, $\text{YCu}^{\text{III}}\text{O}_3$ with the perovskite structure may be prepared under high oxygen pressure. In the $\text{La}_{1+y}\text{Ba}_{2-y}\text{Cu}_3\text{O}_{6+x}$ system, *x* values in excess of 1.0 can be achieved and apparently cannot be avoided as *y* increases. This extra oxygen beyond *x* = 1.0 must bond the Cu–O chains together bringing some of the chain copper coordination to five or six or both.

Many substitutions into $\text{YBa}_2\text{Cu}_3\text{O}_7$ have been attempted. Some have been successful; none have increased T_c . Almost any rare earth may be substituted for Y, and there is very little change in properties. Neither Ce nor Tb have been substituted for La, presumably because both Ce and Tb have a stable tetravalent state. Although $\text{PrBa}_2\text{Cu}_3\text{O}_7$ has been prepared with the $\text{YBa}_2\text{Cu}_3\text{O}_7$ structure, it is not superconducting. This lack of superconductivity is likely related to the $\text{Cu}^{\text{III}} + \text{Pr}^{\text{III}} \rightleftharpoons \text{Cu}^{\text{II}} + \text{Pr}^{\text{IV}}$ couple.

Substitutions into $\text{YBa}_2\text{Cu}_3\text{O}_7$ for Ba have been successful with Sr and some of the larger rare earths, especially La. All these substitutions result in lowered T_c with eventual loss of superconducting properties. There have been many partial substitutions for Cu, both transition metals and nontransition metals. In all cases, T_c drops and superconductivity ultimately disappears.

The only anion that could be expected to substitute for oxygen and support the trivalent state for copper is fluorine. However, there are no examples of electron delocalization through the fluoride anion. Thus, although fluorine substitutions for oxygen have succeeded (33), the superconducting properties are degraded as expected. There are some reports of sulfur substitution for oxygen, but these are not convincing. Furthermore, Cu^{III} cannot exist in the presence of S^{2-} ; thus, sulfides of copper would not appear promis-

Table 2. Summary for $(\text{AO})_m\text{M}_2\text{Ca}_{n-1}\text{Cu}_n\text{O}_{2n+2}$ phases.

Compound	<i>a</i> (Å)	<i>c</i> (Å)	T_c (K)
$\text{TlBa}_2\text{CuO}_5$	3.83	9.55	*
$\text{TlBa}_2\text{CaCu}_2\text{O}_7$	3.833	12.68	90
$\text{TlBa}_2\text{Ca}_2\text{Cu}_3\text{O}_9$	3.853	15.91	110
$\text{TlBa}_2\text{Ca}_3\text{Cu}_4\text{O}_{11}$	3.850	19.01	122
$(\text{Tl,Bi})\text{Sr}_2\text{CuO}_5$	3.745	9.00	50
$(\text{Tl,Bi})\text{Sr}_2\text{CaCu}_2\text{O}_7$	3.800	12.07	90
$(\text{Tl,Pb})\text{Sr}_2\text{CaCu}_2\text{O}_7$	3.800	12.15	90
$(\text{Tl,Pb})\text{Sr}_2\text{Ca}_2\text{Cu}_3\text{O}_9$	3.808	15.23	122
$\text{Tl}_2\text{Ba}_2\text{CuO}_6$	3.866	23.24	90
$\text{Tl}_2\text{Ba}_2\text{CaCu}_2\text{O}_8$	3.855	29.42	110
$\text{Tl}_2\text{Ba}_2\text{Ca}_2\text{Cu}_3\text{O}_{10}$	3.849	35.66	122
$\text{Bi}_2\text{Sr}_2\text{CuO}_6$	3.796	24.62	12
$\text{Bi}_2\text{Sr}_2\text{CaCu}_2\text{O}_8^\dagger$	3.823	30.90	90
$\text{Bi}_2\text{Sr}_2\text{Ca}_2\text{Cu}_3\text{O}_{10}^\dagger$	3.818	37.88	110

*Not superconducting. †Cell dimensions are for an idealized subcell.

ing for superconductivity. However, we must remember that both $\text{CuS} [\text{Cu}_2^{\text{II}}(\text{S}_2)^{-\text{II}}(\text{S}_2)^{-\text{II}}]$ and $\text{CuS}_2 [\text{Cu}^{\text{II}}(\text{S}_2)^{-\text{II}}]$ are superconducting both with T_c 's of about 1.6 (34, 35).

$\text{YBa}_2\text{Cu}_4\text{O}_8$ and $\text{Y}_2\text{Ba}_4\text{Cu}_7\text{O}_{15}$

The $\text{YBa}_2\text{Cu}_4\text{O}_8$ phase was first detected by electron microscopy (36) as an intergrowth in $\text{YBa}_2\text{Cu}_3\text{O}_7$. Later, single-phase $\text{YBa}_2\text{Cu}_4\text{O}_8$ was prepared as a thin film on a SrTiO_3 substrate (37). The structure solved from x-ray diffraction on a thin film (38) was shown to be similar to the structure of $\text{YBa}_2\text{Cu}_3\text{O}_7$. The chains in $\text{YBa}_2\text{Cu}_3\text{O}_7$ consist of CuO_4 units that share corners. However, in $\text{YBa}_2\text{Cu}_4\text{O}_8$, the chains are formed from CuO_4 units that share edges to form double chains. Recently (39), there has been success in preparing bulk $\text{RBa}_2\text{Cu}_4\text{O}_8$ phases where R can be a variety of the rare earths and the T_c 's range from 57 to 81 K.

Investigation of the Y/Ba/Cu/O system at high pressure led to the discovery of $\text{Y}_2\text{Ba}_4\text{Cu}_7\text{O}_{15}$ (40) with a T_c of about 40 K. The structure may be viewed as a 1:1 ordered intergrowth of $\text{YBa}_2\text{Cu}_3\text{O}_7$ plus $\text{YBa}_2\text{Cu}_4\text{O}_8$. The same structure has been found for $\text{Yb}_2\text{Ba}_4\text{Cu}_7\text{O}_{15}$ ($T_c \sim 86$ K) prepared by oxidizing a Yb/Ba/Cu alloy (41).

Thallium-, Lead-, and Bismuth-Copper-Oxide Superconductors

Many of the most recently discovered superconductors may be represented as $(\text{AO})_m\text{M}_2\text{Ca}_{n-1}\text{Cu}_n\text{O}_{2n+2}$ where M may be Ba or Sr. The cation (A) may be Tl, Bi, a mixture of Bi and Pb (42), Bi and Tl (43), or Tl and Pb (44) (Table 2). The structures contain the Cu–O sheets of Fig. 3, and the number of such copper sheets which have stacked consecutively is indicated by *n*. The number of consecutively stacked AO sheets is indicated by *m*, which may be 1 or 2 for A = Tl but only 2 for A = Bi. The environment of the A cation is highly distorted octahedral. There may be some substitution for Ca by Sr or Y. For *n* = 0, there is no Ca and the structure is a single Cu–O layer structure very similar to the La_2CuO_4 structure. There is no *n* = 0 phase, but $(\text{Ca,Sr})\text{CuO}_2$ is the *n* = ∞ phase, which is not superconducting (45).

In the $(\text{TlO})_2\text{Ba}_2\text{Ca}_{n-1}\text{Cu}_n\text{O}_{2n+2}$ series, the structures (Fig. 5) for *n* = 1, 2, and 3 have been well determined from both single-crystal x-ray diffraction data and neutron powder diffraction data (46, 47). The structures with *n* = 2 and 3 have tetragonal symmetry with an *a* axis of 3.85 Å. For *n* = 1, both tetragonal and orthorhombic

symmetry have been observed at room temperature (48), indicating a range of stoichiometry for this phase. As the degree of orthorhombic distortion increases, T_c decreases eventually leading to a nonsuperconducting insulator (49). With an increasing number of copper layers, the c axis increases and T_c increases (Table 2). Electron microscopy studies show regions with $n = 5$, and these may be responsible for superconducting onset behavior at about 140 K. The highest value of zero resistivity reported in the Tl/Ba/Ca/Cu/O system is 122 K. In the $(\text{TlO})_1\text{Ba}_2\text{Ca}_{n-1}\text{Cu}_n\text{O}_{2n+2}$ series, electron microscopy evidence for $n = 1, 2$, and 3 phases has been given (50), and the $n = 2$ phase has been synthesized as nearly a single phase (51). However, only the structure of the $n = 3$ phase ($T_c \sim 110$ K) has been well determined from single crystal diffraction studies (52). The $n = 4$ and $m = 1$ phase has also been reported with a T_c of 122 K (43). The $(\text{TlO})_m\text{Ba}_2\text{Ca}_{n-1}\text{Cu}_n\text{O}_{2n+2}$ phases have given us high T_c examples with tetragonal symmetry and flat Cu–O sheets. However, there are highly correlated displacements of atoms within the Tl–O sheets such that the true local symmetry is not tetragonal (53).

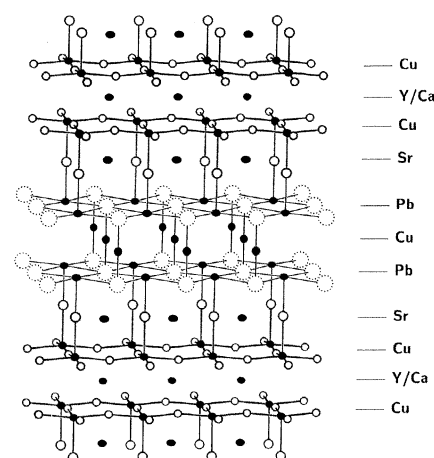
For the $(\text{BiO})_2\text{Sr}_2\text{Ca}_{n-1}\text{Cu}_n\text{O}_{2n+2}$ series, only the $n = 1$ and 2 phases have been prepared as crystals or well-crystallized single-phases (47, 54). However, heating periods of about one week can produce a nearly single phase material with $n = 3$. This poorly crystalline product has a T_c close to 110 K.

The structures of $(\text{BiO})_2\text{Sr}_2\text{Ca}_{n-1}\text{Cu}_n\text{O}_{2n+2}$ phases are much more complicated than those of the analogous Tl–Ba phases. The symmetry has dropped to orthorhombic or possibly lower. There are now complex superstructures that are incommensurate with the primary subcells. These superstructures are related to displacements in the Bi–O layers along both the a and c axes (55, 56). These displacements appear to create a typical Bi^{III} coordination with three short Bi–O distances of about 2.2 Å. The wave created in the Bi–O sheets also results in static wave formation in the CuO_2 sheets (55). Some substitution of Sr for Ca occurs such that the $n = 2$ phase should be formulated as $(\text{BiO})_2\text{Sr}_{3-x}\text{Ca}_x\text{Cu}_2\text{O}_6$ (54, 57). The incommensurate modulation in these phases is not very sensitive to cation or anion stoichiometry although another modulation has also been reported (58).

The pseudo-tetragonal symmetry of the orthorhombic $(\text{BiO})_2\text{Sr}_2\text{Ca}_{n-1}\text{Cu}_n\text{O}_{2n+2}$ phases gives rise to the possibility of the 110 twinning so prevalent in $\text{YBa}_2\text{Cu}_3\text{O}_7$. In fact such twinning is not common in these bismuth phases, but a 90° misorientation defect is common in both $\text{YBa}_2\text{Cu}_3\text{O}_7$ and $(\text{BiO})_2\text{Sr}_2\text{Ca}_{n-1}\text{Cu}_n\text{O}_{2n+2}$ phases. This is distinct from twinning in that it causes strain instead of relieving it. In the $(\text{BiO})_2\text{Sr}_2\text{Ca}_{n-1}\text{Cu}_n\text{O}_{2n+2}$ phases, this 90° misorientation defect is largely a stacking defect whereby the a and b axes interchange along the c axis direction. Such a defect is expected to be highly pronounced in view of the pseudotetragonal symmetry with a and b cell edges that are nearly identical.

The formula $(\text{A}^{\text{III}}\text{O})_2\text{M}^{\text{II}}\text{Ca}_{n-1}\text{Cu}_n\text{O}_{2n+2}$ is an ideal one and does not allow for the presence of Cu^{III} . Based on our understanding of copper-oxide superconductors, we are compelled to find evidence for Cu^{III} . In fact, chemical analysis of the $n = 1$ and 2 phases where A^{III} is Bi indicates the presence of Cu^{III} (54). Thus, it was initially proposed that there are oxygen interstitials, for example in $(\text{BiO})_2\text{Sr}_2\text{CaCu}_2\text{O}_{6+y}$, and recent structural evidence has been found for such interstitial oxygen in some, but not all, crystals (59). However, such interstitials between adjacent BiO layers result in decreased T_c . It appears that Cu^{III} might also result from a deficiency at the Sr sites, that is $(\text{BiO})_2\text{Sr}_{2-x}\text{CaCu}_{2-2x}\text{Cu}_{2x}^{\text{III}}\text{O}_6$ (60) or a deficiency on the Bi site (55). Another type of defect that could give Cu^{III} is suggested by the observation that Tl and Ca substitute on each others' sites. Thus, Cu^{III} could be created according to $\text{Tl}_{2-x}\text{Ca}_x\text{Ba}_2\text{Ca}_2\text{Cu}_3^{\text{II}}\text{Cu}_x^{\text{III}}\text{O}_8$. Still another mechanism for Cu^{III}

Fig. 6. The structure of $\text{Pb}_2\text{Sr}_2(\text{Ca},\text{Y})\text{Cu}_3\text{O}_8$. Metal atoms are shaded; Cu–O and Pb–O bonds are shown. Oxygen atoms in the PbO sheets are dotted because they are not localized on the ideal sizes.



production in the case of the Tl phases would be the partial oxidation of Cu^{II} by Tl^{III} . The $(\text{TlO})_1\text{Ba}_2\text{Ca}_{n-1}\text{Cu}_n\text{O}_{2n+2}$ phases would normally be formulated as $(\text{Tl}^{\text{III}}\text{O})\text{Ba}_2^{\text{II}}\text{Ca}_{n-1}^{\text{II}}\text{Cu}_{n-1}^{\text{II}}\text{O}_{2n+2}$. This then suggests a higher concentration of Cu^{III} which in turn might be expected to lead to higher T_c 's. Since higher T_c 's are not observed (Table 2), it would seem that the concentration of Cu^{III} is more related to defects and the presence of the Tl 6s band at the Fermi level.

Although the $(\text{A}^{\text{III}}\text{O})_2\text{M}_2^{\text{II}}\text{Ca}_{n-1}\text{Cu}_n\text{O}_{2n+2}$ phases for $\text{A}^{\text{III}} = \text{Tl}$ and Bi are very similar to each other, there are important differences. The bismuth compounds are much more layer-like and have a pronounced micaceous nature. This is undoubtedly related to the lone pair of electrons ($6s^2$) on Bi^{III} which are not present in Tl^{III} . This lone pair of electrons normally hybridizes with the $6p$ levels and moves off to one side of the Bi^{III} cation thus forcing very weak bonds to oxygen on that side. For these layered bismuth compounds, we may then assume that the lone pairs of many Bi^{III} cations are pointed essentially in the direction of the interlayer spacing between the two adjacent Bi/O layers. Thus, these layers are far apart (3.2 Å) and only weakly bonded to each other. The analogous Tl/O layers have much shorter interlayer spacings (2.0 Å) and thus are much more strongly bound to each other. This also means that electron delocalization along the c axis is much easier in the Tl relative to the Bi phases.

Another new series of superconductors can be represented by the formula $\text{Pb}_2\text{Sr}_2(\text{Ca},\text{R})\text{Cu}_3\text{O}_{8+y}$ where R can be a variety of rare earths (61, 62). Although onset behavior in this series has been noted at temperatures as high as 77 K, zero resistance has not yet been found at temperatures higher than 55 K (62). The structure for this new series (Fig. 6) shows the presence of the familiar CuO_2 sheets, two such layers being stacked consecutively. The PbO layers are joined by the $\text{O}-\text{Cu}^{\text{I}}-\text{O}$ sticks found also in $\text{YBa}_2\text{Cu}_3\text{O}_6$. This new system thus represents a second system where superconductivity exists for an average copper oxidation state less than two. However, in both cases, it seems safe to assume that the average oxidation state for copper in the CuO_2 sheets is greater than two.

Correlations with T_c

Various correlations between material properties and T_c have developed as oxide superconductors have been so intensively studied. Some of these correlations are so interdependent that it is difficult to ferret out the truly meaningful correlations. Very early in the investigation of copper-oxide superconductors, it was recognized that T_c increases with decreasing Cu–O distance for the $\text{La}_{2-x}\text{A}_x\text{CuO}_4$ superconductors (63). This increase in T_c could be

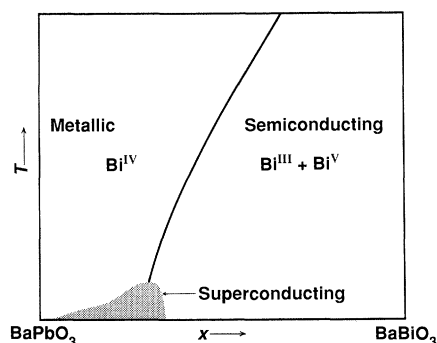


Fig. 7. Schematic phase diagram for $\text{BaPb}_{1-x}\text{Bi}_x\text{O}_3$. Vertical axis is temperature.

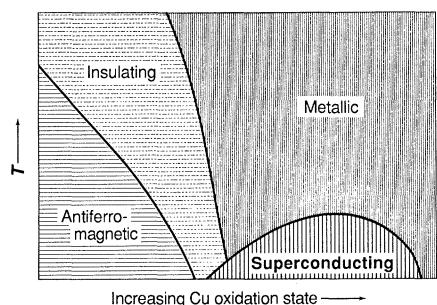


Fig. 8. Antiferromagnetism and superconductivity for $\text{La}_{2-x}\text{A}_x\text{CuO}_4$, $\text{YBa}_2\text{Cu}_3\text{O}_{6+x}$ and $\text{Bi}_{2-x}\text{Sr}_x\text{Cu}_2\text{O}_8$ systems. Vertical axis is temperature.

observed with the application of pressure (64). Also, the A cation substitution of Ba, Sr, Ca, or Na caused a decreased Cu–O distance and an increase in T_c (24, 63). However, in this case increasing x in $\text{La}_{2-x}\text{A}_x\text{CuO}_4$ also increases the Cu^{III} content or the carrier concentration, and there is in general a correlation of higher T_c for higher Cu^{III} content. A higher Cu^{III} content actually causes a decreased Cu–O distance because a $\text{Cu}^{\text{III}}\text{--O}$ distance is shorter than a $\text{Cu}^{\text{II}}\text{--O}$ distance owing to the removal of antibonding electrons from the Cu–O bond. Nonetheless, the high-pressure studies show that decreasing the Cu–O distance increases T_c without increasing the Cu^{III} content. Another correlation with T_c is covalency of Cu–O bonds (19), but again this is highly correlated with the Cu–O distance. Although T_c increases with the number of adjacent CuO_2 layers in any given $(\text{A}^{\text{III}}\text{O})_m\text{A}_2^{\text{II}}\text{Ca}_{n-1}\text{Cu}_n\text{O}_{2n+2}$ series, the Cu–O distance also decreases with increasing n .

(Ba,K) (Bi,Pb)O₃ Superconductors

The $\text{BaPb}_{1-x}\text{Bi}_x\text{O}_3$ system (8) represents a classic case of superconductivity occurring at the metal-to-insulator boundary (Fig. 7). Metallic properties are observed for BaPbO_3 , presumably because it is a zero-gap semiconductor; that is, the “empty” Pb 6s band has overlapped the “filled” O 2p band. On the other hand, BaBiO_3 is a semiconductor even though one might have expected metallic properties attributable to a half-filled 6s band. Both BaPbO_3 and BaBiO_3 possess perovskite structures although the symmetry is always lower than cubic, at least at room temperature and below. Essentially, a complete solid solution can be formed between BaPbO_3 and BaBiO_3 , although at equilibrium there are presumably two-phase regions that would become significant at lower temperatures if equilibrium were achieved.

With increasing x in the $\text{BaPb}_{1-x}\text{Bi}_x\text{O}_3$ system, electrons are added to the 6s band composed of Bi 6s, Pb 6s, and O 2p states. There is already superconductivity at $x = 0$ (that is BaPbO_3), but the T_c is only 0.5 K (65). As x increases the T_c increases, reaching a maximum of about 13 K at $x = 0.27$. With a further increase in x , T_c rapidly drops and the properties become semiconducting. For

the highest values of x for which superconductivity is observed ($x \sim 0.3$), there is a semiconductor-to-superconductor transition in accordance with Fig. 7. These semiconductor-to-insulator transitions are also observed for the copper-oxide superconductors. Whether such transitions are intrinsic properties of homogeneous materials, or are instead related to inhomogeneities intrinsic to any solid solution, remains an unsettled issue.

The compositions from $\text{BaPb}_{0.7}\text{Bi}_{0.3}\text{O}_3$ to BaBiO_3 are all insulating for reasons that become clear on examination of the structure of BaBiO_3 . Neutron diffraction studies (66) show two types of Bi in BaBiO_3 which may be designated as Bi^{III} and Bi^{V} . This interpretation does not imply a real charge difference of two at the different Bi sites. In fact, the covalency is so high in this system that the real charges of both Bi^{III} and Bi^{V} are much reduced. The $\text{Bi}^{\text{III}}\text{--O}$ distances are longer than $\text{Bi}^{\text{V}}\text{--O}$ distances because the σ antibonding 6s electron density has been removed from the $\text{Bi}^{\text{V}}\text{--O}$ bond and localized in the $\text{Bi}^{\text{III}}\text{--O}$ band. Thus, this disproportionation of Bi^{III} into Bi^{III} and Bi^{V} causes pairing of the 6s electrons. Many analogous situations are well known in Sb chemistry where the mixed $\text{Sb}^{\text{III}}\text{--Sb}^{\text{V}}$ oxidation states are verified by Mossbauer spectroscopy. Thus, the insulating properties of BaBiO_3 are understood. The chemist's description of disproportionated $\text{Ba}_2\text{Bi}^{\text{III}}\text{Bi}^{\text{V}}\text{O}_6$ is fully equivalent to the physicist's description of a charge density wave in BaBiO_3 where the charges on the two inequivalent bismuth cations are both much lower than the formal oxidation state values. Recent muon experiments have confirmed that BaBiO_3 is not antiferromagnetic $\text{BaBi}^{\text{IV}}\text{O}_3$ (67).

In the metallic region of the $\text{BaPb}_{1-x}\text{Bi}_x\text{O}_3$ system, the bismuth oxidation state is given as Bi^{IV} because the 6s electrons are delocalized. However, with increasing x the tendency of Bi^{IV} to disproportionate increases. Beyond $x = 0.3$, this disproportionation of Bi^{IV} into Bi^{III} and Bi^{V} has largely occurred, resulting in localized electron properties. The long-range ordering of Bi^{III} and Bi^{V} does not occur because of the disruption of the lattice caused by having Pb on “Bi sites”. The question that I will come back to in the next section is whether the tendency of Bi^{IV} to disproportionate at low x values is directly related to superconductivity.

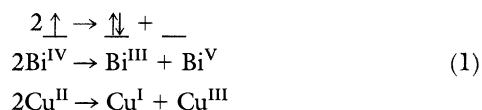
Many substitutions into $\text{BaPb}_{1-x}\text{Bi}_x\text{O}_3$ were attempted about fifteen years ago. None produced higher T_c 's although alkali substitution for Ba, as in $\text{Ba}_{1-y}\text{K}_y\text{Pb}_{1-x}\text{Bi}_x\text{O}_3$ for instance, did promote stronger and sharper transitions (8). An obvious analogy to the $\text{BaPb}_{1-x}\text{Bi}_x\text{O}_3$ system would be $\text{Ba}_{1-x}\text{K}_x\text{BiO}_3$. This was also attempted in the mid-1970s, but no evidence of superconductivity was found. However, with appropriate synthesis conditions (14), superconductors with T_c 's of 29 K may be obtained. Very recently (68), the T_c in the (Ba,K)BiO₃ system has been pushed up to 34 K.

Mechanisms for Superconductivity

The recent dramatic increases of T_c have given reason to believe that some totally new mechanism for superconductivity is operating in the oxides of Cu and Bi. Indeed there is certainly something new at work in these oxide superconductors. However, it is known that the electrons responsible for superconductivity are still paired with spins antiparallel as in the traditional BCS theory of superconductivity. Before the advent of the high T_c oxide superconductors, it was believed that this electron pairing was always mediated by an electron-phonon interaction, which had been verified in some cases by studying the variation of T_c with isotopic substitution. Since the isotope effect on T_c for $\text{YBa}_2\text{Cu}_3\text{O}_7$ is extremely small, the electron-phonon coupling mechanism for superconductivity has been questioned for this type of material. However, it is theoretically known that the isotope effect on T_c can disappear for a strong electron-

phonon interaction. Thus, it is possible that a unique aspect of the new high T_c superconductors is a very strong electron-phonon coupling. One current problem with this approach is identifying the phonon involved. The only soft phonon so far found in these materials is associated with bending the Cu–O–Cu bond (23) and it appears that this mode does not couple sufficiently to the conduction electrons to result in a mechanism for high T_c .

One significant conclusion about the new oxide superconductors is that there is a short coherence length for the electron pair; thus, we may think of this pair as existing in real space instead of momentum space. An example of a real-space mechanism for superconductivity would be disproportionation of a certain type:



These spin-pairing disproportionation reactions can lead to electron localization as well as superconductivity (19, 69, 70). In fact, it appears always necessary to dilute the \uparrow states with the empty $_$ state to prevent the complete disproportionation to the insulating state. It should be noted that this mechanism only works for the d^9 situation if the degeneracy between the d_{z^2} and $d_{x^2-y^2}$ levels is lifted as happens for square planar copper. Thus, one prediction of this mechanism is that superconductivity will not occur for octahedral copper. In fact, the LaCuO_{3-x} perovskite containing octahedral copper is metallic but not superconducting. Octahedral copper presumably forms in the $\text{La}_{1+y}\text{Ba}_{2-y}\text{Cu}_3\text{O}_{6+x}$ system for x values greater than one and could then be the reason why superconductivity disappears. This model for superconductivity can be applied to nearly all known oxide superconductors as well as all the superconductors based exclusively on post-transition elements, SnP for instance. Although the disproportionation mechanism may be viewed as a nonphonon mechanism for superconductivity (70, 71), it appears more likely that it in fact is related to strong coupling of a breathing mode phonon to the conduction electrons. For both the Cu- and Bi-based oxide superconductors, the conduction band is sigma antibonding in character, which might then give rise to an especially strong electron-phonon coupling.

Other real-space mechanisms for spin pairing can be referred to as magnetic-like. That is, electrons on different sites are paired through the same type of interactions that can give rise to magnetic order. We know for example that the 180° $\text{Cu}^{\text{II}}\text{--O--Cu}^{\text{II}}$ linkage tends to couple the spins on Cu^{II} antiparallel, which then gives an antiferromagnetic structure in, for example, La_2CuO_4 . We further know that the magnetic ordering temperature (T_N) in both the $\text{La}_2\text{CuO}_{4-x}$ and $\text{YBa}_2\text{Cu}_3\text{O}_{6+x}$ systems decreases as we approach the superconducting state (72, 73). Locally however, there will still be a tendency for spin pairing between Cu^{II} cations that could be the spin pairing required for superconductivity. A schematic phase diagram is then suggested for copper oxide systems that exhibit both antiferromagnetism and superconductivity (Fig. 8). As the copper oxidation state increases, the magnetic ordering temperature (T_N) decreases. Soon after T_N reaches 0 K, superconductivity appears and T_c increases with increasing Cu^{III} content. Ultimately, there is saturation and T_c decreases. This behavior is also observed in the $\text{Bi}_2\text{Sr}_{3-x}\text{Y}_x\text{Cu}_2\text{O}_8$ system (74, 75).

We can also consider the possibility that the electrons that pair to give superconductivity reside mostly on oxygen. Thus, we are considering formally the species O^{-1} , a species which is completely unknown in concentrated systems. However O^{-1} could be viewed as existing as a dilute and mobile species in a $\text{Cu}^{\text{II}}\text{--O}^{\text{II}}$ lattice. Several mechanisms for spin pairing these O^{-1} species have been proposed as mechanisms for superconductivity (21, 30, 76, 77).

All the copper oxide-based superconductors apparently have holes in the conduction band that could be represented as Cu^{III} or O^{-1} . Without any intent to distinguish between these two possibilities, I have adopted the usual chemistry convention and referred to these holes as Cu^{III} . Without holes, as in La_2CuO_4 , the materials are antiferromagnetic insulators with no superconductivity. The holes may be introduced into the Cu–O sheets in various ways. The common way in $\text{La}_2\text{Cu}^{\text{II}}\text{O}_4$ is to dope a lower valent cation on the La site, as for instance in $\text{La}_{2-x}\text{Sr}_x\text{Cu}^{\text{II}}_{1-x}\text{Cu}^{\text{III}}_x\text{O}_4$. For $\text{YBa}_2\text{Cu}_3\text{O}_{6+x}$ phases, holes develop in the Cu–O sheets as x increases and the Cu–O chains form. Indeed the only important role of the chains may be that their formation results in Cu^{III} in the Cu–O sheets (78).

A very interesting possibility for creating Cu^{III} exists with the $(\text{A}^{\text{III}}\text{O})_m\text{A}^{\text{II}}\text{Ca}_{n-1}\text{Cu}_n\text{O}_{2n+2}$ phases where A^{III} is Bi or Tl. The oxides PbO_2 , BaPbO_3 and Tl_2O_3 all formally should be semiconductors with a filled oxygen $2p$ band and an empty $6s$ conduction band. However, they are black materials with metallic properties and it is apparent that $6s$ and $2p$ bands are overlapped. Thus, in $(\text{TlO})_m\text{Ba}_2\text{Ca}_{n-1}\text{Cu}_n\text{O}_{2n+2}$ phases we may expect that the Tl $6s$ band overlaps the Cu $3d$ band at the Fermi level. This is the same as oxidation of Cu^{II} by Tl^{III} . Thus, some Cu^{III} is produced and there are electrons in the Tl $6s$ band making the $(\text{TlO})_m\text{Ba}_2\text{Ca}_{n-x}\text{Cu}_n\text{O}_{2n+2}$ phases good conductors in all three dimensions. In fact, the partially filled $6s$ band should promote superconductivity just as in $\text{BaPb}_{1-x}\text{Bi}_x\text{O}_3$.

Band structure calculations on $\text{Bi}_2\text{Sr}_2\text{CaCu}_2\text{O}_8$ have indicated that the Bi $6p$ band also overlaps the Cu $3d$ band at the Fermi level (79). However, this is chemically unreasonable because it is akin to oxidation of Cu^{II} by Bi^{III} which would not normally occur. This is not to say the band-structure calculation is incorrect for the structure assumed. The real structure for $\text{Bi}_2\text{Sr}_2\text{CaCu}_2\text{O}_8$ significantly differs from the ideal structure in having shorter Bi–O distances that would cause the Bi $6p$ band to move up away from the Fermi level. Recent resonance inverse photoemission data also place the Bi $6p$ band well above the Fermi level (80). This is not to say, however, that there are not Bi $6p$ or Bi $6s$ states at the Fermi level as a result of covalency effects. One must still consider the possibility of a Bi $6s$ -type band at the Fermi level as occurs in the $\text{BaPb}_{1-x}\text{Bi}_x\text{O}_3$ system. To answer this question we need to know the exact structure and composition of “ $\text{Bi}_2\text{Sr}_2\text{CaCu}_2\text{O}_8$ ”. If there is some tendency for Cu^{III} to oxidize Bi^{III} , this could result in a Bi $6s$ band at the Fermi level.

Conclusion

The new high-temperature superconductors are not currently understood, but there is much optimism that the essential understanding will emerge within the next year. The chemistry and physics of these materials have been fascinating in numerous ways. For condensed matter science, the best scientific minds of the world are being challenged in an unprecedented manner.

Lacking a mechanistic understanding, we can develop guidelines based on current observations and correlations (81). Such guidelines or rules can lead to the discovery of new compounds as well as lay the basis for theoretical understanding. One guideline has been that superconductivity tends to occur at the boundary between localized and delocalized electron behavior. Various mechanistic approaches would suggest that the same basic mechanism can cause either superconductivity or electron localization. With this in mind, it is not surprising that superconductors above their T_c have anomalous properties and are not good metals.

Another characteristic of oxide superconductors is that they all contain mixed-valent cations. It would even seem that three oxidation states need to be accessible; for example, Bi^{III} , Bi^{IV} and Bi^{V} or

Cu^I, Cu^{II} and Cu^{III}. This is of course a requirement of the disproportionation mechanisms for superconductivity. This is also the same as saying that we are always dealing with a band that becomes filled with just two electrons, and that there is some extra stability at the empty, half-filled and completely filled levels. Such bands are rare; *s* bands are our best examples. For *d* bands, this situation arises for the *d*⁹ situation when the symmetry is noncubic. It can also occur for low-symmetry *d*¹ situations (17).

Magnetic interactions have historically been considered destructive of superconductivity. Certainly, as the number of unpaired electrons per cation increases above one, superconductivity usually disappears, presumably because magnetism then dominates superconductivity.

High-temperature superconductivity only occurs in oxides where there is very high covalency. In part, we can simply say that this covalency is necessary to develop bands capable of supporting metallic behavior. Thus, we might be able to develop all other conditions for superconductivity, such as appropriate mixed valency, but the system would simply be too ionic to allow delocalized electron behavior. Conversely, a very broad conduction band might be expected to produce only low *T*_c superconductors.

Basic or electropositive cations such as Ba^{II} and the La^{III} seem to help in the formation of superconducting oxides. In part, this may be simply that they make certain Cu–O networks possible; for example, networks with 180° Cu–O–Cu connections. However, these electropositive cations have other effects that seem to be important. They increase the covalency of the Cu–O bond (17). They also stabilize high oxidation states of cations, Cu^{III} and Bi^V, for example. This is actually an indirect effect; the basic cations so stabilize the O 2*p* levels that high oxidation states are possible (17).

On the basis of our guidelines for superconductivity, we can expect to see *T*_c's continue to rise somewhat for Cu–O systems. Certainly, we can expect to discover new superconducting systems that are not based on copper and oxygen. However, we have no way to predict which new discoveries might lead to even higher *T*_c.

REFERENCES AND NOTES

1. T. H. Geballe and J. K. Hulm, *Science* **239**, 367 (1988).
2. J. K. Hulm, C. K. Jones, R. Mazelsky, R. A. Hein, J. W. Gibson, In *Proceedings of the 9th International Conference on Low Temperature Physics*, J. G. Daunt, D. O. Edwards, F. J. Milford, M. Yaqub, Eds. (1965), pp. 600–604; there is actually a range of TiO_x composition with varying *T*_c's.
3. J. J. Schooley, W. R. Hosler, M. L. Cohen, *Phys. Rev. Lett.* **12**, 474 (1964).
4. A. R. Sweedler, C. Raub, B. T. Matthias, *Phys. Lett.* **15**, 108 (1965).
5. A. W. Sleight, T. A. Bither, P. E. Bierstedt, *Solid State Commun.* **7**, 299 (1969).
6. M. B. Robin, K. Andres, T. H. Geballe, N. A. Kuebler, D. B. McWhan, *Phys. Rev. Lett.* **17**, 917 (1966).
7. D. C. Johnston, H. Prakash, W. H. Zachariasen, R. Viswanathan, *Mater. Res. Bull.* **8**, 777 (1973).
8. A. W. Sleight, J. L. Gillson, P. E. Bierstedt, *Solid State Commun.* **17**, 27 (1975).
9. J. G. Bednorz and K. A. Müller, *Z. Phys.* **B64**, 189 (1986).
10. M. K. Wu *et al.*, *Phys. Rev. Lett.* **58**, 908 (1987).
11. C. Michel *et al.*, *Z. Phys.* **B68**, 421 (1987).
12. H. Maeda *et al.*, *Jpn. J. Appl. Phys.* **27**, L209 (1988).
13. Z. Z. Sheng and A. M. Herman, *Nature* **332**, 55 (1988).
14. L. F. Mattheiss, E. M. Gyorgy, D. W. Johnson, *Phys. Rev. B* **37**, 3745 (1988); R. J. Cava *et al.*, *Nature* **332**, 814 (1988).
15. The Ti–Ti distance of 2.97 Å in LiTi₂O₄ might be considered short enough for a significant interaction. This is a borderline situation where it is questionable whether or not electron delocalization could occur without admixture of oxygen 2*p* states into the conduction band.
16. The only exception is A_xReO₃ superconductors where there are 1 + *x* 5*d* electrons per Re.
17. A. W. Sleight, in *High-Temperature Superconducting Materials*, W. E. Hatfield and J. H. Miller, Eds. (Dekker, NY, 1988), pp. 1–36.
18. Tetrahedral Cu^I is well known in halides and sulfides of copper. Also, an irregular coordination of Cu^I by four O^{2–} is known, for example, in Cu₆Mo₅O₁₈ and Cu₄Mo₅O₁₇, E. M. McCarron, J. C. Calabrese, *J. Solid State Chem.* **62**, 64 (1986) and *ibid.* **65**, 215 (1986).
19. A. W. Sleight, in *Chemistry of High-Temperature Superconductors*, D. L. Nelson, M. S. Whittingham, T. F. George, Eds. (American Chemical Society, Washington, DC, 1987), pp. 2–12.
20. H. Verweij, *Solid State Commun.* **64**, 1213 (1987); D. Ahyja, *Mat. Res. Soc. Symp. Proc.* **99**, 467 (1988); M.-Y. Su, S. E. Davis, T. O. Mason, *J. Solid State Chem.* **75**, 381 (1988).
21. Y. Guo, J.-M. Langlois, W. A. Goddard III, *Science* **239**, 896 (1988).
22. J. Gopalakrishnan *et al.*, in preparation.
23. R. J. Birgeneau *et al.*, *Phys. Rev. Lett.* **59**, 1329 (1987).
24. M. A. Subramanian *et al.*, *Science* **240**, 495 (1988).
25. M. A. Dixon, P. D. VerNooy, A. M. Stacy, in *High Temperature Superconductors II*, D. W. Capone, W. H. Butler, B. Battlogg, C. W. Chu, Eds. (Materials Research Society, Pittsburgh, PA 1988), pp. 69–73.
26. A. W. Sleight, M. A. Subramanian, U. Chowdhry, in preparation.
27. H. S. Horowitz *et al.*, *Science*, in press.
28. R. J. Cava *et al.*, *Nature* **329**, 423 (1987).
29. M. A. Alario-Franco *et al.*, *Mater. Res. Soc. Symp. Proc.* **99**, 41 (1988).
30. J. B. Goodenough, *Mater. Res. Bull.* **23**, 401 (1988).
31. J. A. Gardner *et al.*, *Phys. Rev. B*, in press.
32. E. M. McCarron *et al.*, *Mater. Res. Soc. Proc.* **99**, 101 (1988).
33. P. Davies *et al.*, *Solid State Commun.* **64**, 1441 (1987).
34. T. Nakajima, M. Isino, E. Kanda, *J. Phys. Soc. Jap.* **28**, 369 (1970).
35. R. A. Munson, W. DeSorbo, J. S. Kouvel, *J. Chem. Phys.* **47**, 1769 (1967).
36. D. J. Eaglesham *et al.*, *Appl. Phys. Lett.* **51**, 457 (1987); M. P. A. Viegars *et al.*, *J. Mater. Res.* **2**, 743 (1987); J. Narayan *et al.*, *Appl. Phys. Lett.* **51**, 940 (1987); H. W. Zandbergen *et al.*, *Nature* **331**, 596 (1988).
37. A. F. Marshall *et al.*, *Phys. Rev. B* **37**, 9353 (1988).
38. P. Marsh *et al.*, *Nature* **334**, 141 (1988).
39. D. E. Morris *et al.*, in preparation.
40. P. Bordet *et al.*, *Nature* **334**, 596 (1988).
41. T. Kogure *et al.*, *Physica C* **156**, 45 (1988).
42. R. J. Cava *et al.*, *ibid.* **C153–155**, 560 (1988).
43. P. Haldar *et al.*, *Science* **241**, 1198 (1988).
44. M. A. Subramanian *et al.*, *ibid.*, **242**, 249 (1988).
45. T. Siegrist *et al.*, *Nature* **334**, 231 (1988).
46. M. A. Subramanian *et al.*, *ibid.* **332**, 420 (1988); C. C. Torardi *et al.*, *Science* **240**, 631 (1988); D. E. Cox *et al.*, *Phys. Rev. B* **38**, 6624 (1988).
47. C. C. Torardi *et al.*, *Phys. Rev. B* *ibid.* p. 225.
48. J. B. Parise, *J. Solid State Chem.* **76**, 432 (1988).
49. N. Herron *et al.*, in preparation.
50. S. S. P. Parkin *et al.*, *Phys. Rev. Lett.* **61**, 750 (1988).
51. M. Hervieu *et al.*, *Solid State Chem.* **75**, 212 (1988).
52. M. A. Subramanian *et al.*, *ibid.* **77**, 192 (1988).
53. W. Dmowski *et al.*, *Phys. Rev. Lett.* **61**, 2608 (1988).
54. M. A. Subramanian *et al.*, *Science* **239**, 1015 (1988).
55. Y. Gao *et al.*, *ibid.* **241**, 954 (1988).
56. P. Gai and P. Day, *Physica C*, **152**, 335 (1988).
57. G. S. Grader *et al.*, *Phys. Rev.* **B38**, 757 (1988).
58. A. F. Marshall *et al.*, *Appl. Phys. Lett.* **53**, 426 (1988).
59. P. Coppens *et al.*, in preparation; C. C. Torardi *et al.*, *Physica C*, in press.
60. A. K. Cheetham *et al.*, *Nature* **333**, 21 (1988).
61. R. J. Cava *et al.*, *ibid.* **336**, 211 (1988).
62. M. A. Subramanian *et al.*, *Physica C*, in press.
63. K. Fueki, in (17), p. 38.
64. H. Takahashi *et al.*, *Jpn. J. Appl. Phys.* **26**, L504 (1987); S. Yomo *et al.*, *ibid.*, p. 1603.
65. V. V. Bagotko and Yu. N. Venevtsev, *Sov. Phys. Solid State* **22**, 705 (1980).
66. D. E. Cox and A. W. Sleight, *Acta Cryst.* **B35**, 1 (1979).
67. Y. J. Uemura *et al.*, *Nature*, **335**, 151 (1988).
68. N. Jones, R. Flippen, A. W. Sleight, in preparation.
69. T. M. Rice and L. Sneddon, *Phys. Rev. Lett.* **47**, 689 (1981).
70. J. A. Wilson, *J. Phys. C*, **21**, 2067 (1988).
71. J. E. Hirsch and D. J. Scalapino, *Phys. Rev. B* **32**, 5639 (1985).
72. Y. J. Uemura *et al.*, *Phys. Rev. Lett.* **59**, 1045 (1987).
73. J. H. Brewer *et al.*, *ibid.* **60**, 1073 (1988).
74. M. A. Subramanian *et al.*, *J. Solid State Chem.* **77**, 196 (1988).
75. Y. J. Uemura *et al.*, *Journal de Physique (Paris)*, in press.
76. V. J. Emery, *Phys. Rev. Lett.* **58**, 2794 (1987).
77. D. J. Scalapino, E. Loh, J. E. Hirsch, *Phys. Rev. B* **35**, 6694 (1987).
78. Holes in the Cu–O sheets could develop before the average valency in YBa₂Cu₃O_{6+x} reaches two at *x* = 0.5. That is, the average valency of Cu could be less than two in the chains but greater than two in the sheets.
79. M. S. Hybertsen and L. F. Mattheiss, *Phys. Rev. Lett.* **60**, 1661 (1988); H. Krakauer and W. E. Pickett, *ibid.*, p. 1665.
80. T. J. Wagener *et al.*, *Phys. Rev. B*, in press.
81. A. W. Sleight, *Chemtronics* **2**, 116 (1987).
82. I thank C. C. Torardi for preparation of the structural diagrams.